



Supporting Online Material for

Forced Unfolding of Proteins within Cells

Colin P. Johnson, Hsin-Yao Tang, Christine Carag, David W. Speicher,
Dennis E. Discher*

To whom correspondence should be addressed. E-mail: discher@seas.upenn.edu

Published 3 August 2007, *Science* **317**, 663 (2005)
DOI: 10.1126/science.1139857

This PDF file includes

Materials and Methods
SOM Text: Analysis
Figs. S1 to S4
Tables S1 to S2
References and Notes

Supplemental Materials & Methods

Fluorescent dyes and Cell sources All dyes were purchased from Invitrogen (Carlsbad, CA). BODIPY-IA is N-(4,4-difluoro-1,3,5,7-tetramethyl-4-bora-3a,4a-diaza-s-indacene-2-yl) iodoacetamide or BODIPY 507/545 IA. RBCs were obtained by fingerprick from healthy human volunteers, and MSCs were purchased from Cambrex (East Rutherford, NJ).

For the RBC labeling experiments, in brief, blood was centrifuged at 1000 g for 5 minutes, after which the white cells ('buffy coat') were removed to minimize subsequent proteolysis. Pink ghosts were made from the remaining RBC pellet by several cycles of hypotonic lysis and washing in ice cold 5mM PBS (pH 7.4). The ghost pellet was re-suspended in an isotonic 150mM NaCl PBS solution (pH 7.4) containing IAEDANS (Table S1) and allowed to reseal at 37°C for 5 min (eg. An et al, 2002). For single label experiments, 250 μ L of dye-loaded cells were exposed to shear at a constant stress in a cone and plate rheometer (Bohlin Gemini rheometer) or else experimental perturbations such as controlled heating were applied. Both very high dye concentrations (>10 mM) and high shear stresses can disrupt cells; fluorescence and brightfield imaging should be used to verify as here that conditions are not disruptive to cells. For two-dye labeling experiments, the IAEDANS concentration was \sim 250 μ M and dye-loaded cells were incubated at 37°C for 30 minutes and then pelleted. The ghost cell pellet was then re-suspended in a solution of 6 mM BODIPY in isotonic PBS, which was heated to 60°C to increase dye solubility. Cells were then exposed to either static or shear conditions for a set reaction time and temperature. After reaction in both single dye and two-dye experiments, cells were pelleted, lysed in 8M urea with μ M amounts of protease inhibitor cocktail (Sigma) and 50mM beta-mercaptoethanol (β -Me) to quench unreacted dye. The sample was subsequently treated with, an excess of iodoacetamide (IAM) to label unreacted Cys..

Beyond the brief details of labeling given here and in the text, it is important in all such studies to view the many possible Cys reactive probes as pharmacological actives: dose-response behavior (such as spread area in Fig. S4A) should be studied in order to identify regimes in which structural perturbations are minimized. Trace labeling will no doubt be most reliable and push sensitivity limits for detection. While some label-induced perturbations could prove unavoidable and even propagate, they would reasonably shift stresses to other susceptible points in structures and could be reasonably viewed in the context of (oxidatively) accelerated aging. In addition, while the fluorescent dyes tested here are extremely useful as they can be analyzed by all of the various methods presented, better labeling dyes that might improve MS quantitation of ratios could include cleavable fluorophores at the ends of chains as well as heavy and light isotope forms of the probes. Fluorescent probes are not necessary, of course, but they generally provide an accessibility advantage for convenient tracking by densitometry – as available in most labs. The present probes nonetheless provide the first in-cell measurements of force-induced protein unfolding.

SDS-PAGE and densitometry To maximize accuracy in densitometry and ensure that any differences between fluorescence in the *shear* versus static RBC or tensed versus relaxed MSC samples are not due to differences in sample loading, fluorescence values are always normalized by protein staining with Coomassie. In addition, multiple sample loads are analyzed and a standard plot constructed to establish the linearity of the relationship between protein amount and signal. Any differences in the normalized fluorescence intensity for equivalent protein bands between the two samples should thus reflect proportional differences in Cys accessibility due to changes in protein structure. Ratios

proved reproducible within about 10%. To check for labeling-induced perturbations of RBC, Triton-extracted membrane skeletons from dye-treated and untreated samples were examined by SDS-PAGE and showed no significant compositional differences.

Liquid Chromatography Tandem Mass Spectrometry Mass spectrometry (MS) analyses of global post-translational modifications within cells – such as palmitoylation in yeast (Roth 2006) – is becoming increasingly quantitative. Some key recent innovations now allow analysis of large cytoskeletal proteins that extend to quantitation of Cys-IAEDANS modified proteins. Indeed, while it has been feasible to look for modifications of side chains on small proteins for many years using LC-MS/MS or even conventional HPLC, the complexity of such analyses increases dramatically as the size of the target protein increases. For example, most tryptic peptides for a 20-30 kDa protein can be resolved on a high resolution HPLC peptide map, and some but not all stoichiometric modifications in proteins up to 50 kDa can be detected in a reverse phase HPLC separation. In contrast, the tryptic digests of very large proteins such as spectrin (heterodimer = 525 kDa) are so complex (>600 tryptic peptides larger than 500 Da) that even current nanocapillary HPLC interfaced directly with a linear ion trap mass spectrometer (first available 3 years ago) are substantially challenged by such mixtures. The ability to identify substoichiometric modifications in such complex mixtures has been further aided by the availability within the past 2 years of hybrid linear ion trap mass spectrometers with high mass resolution and mass accuracy such as the LTQ FT ICR instrument used in these studies. Finally, while such instrumentations has been available for several years, the high confidence identification of substoichiometric modifications of even modest sized proteins is not routine even for the most expert MS laboratories, and the identification of such modifications on very large proteins such as spectrin remains highly challenging and novel.

For the studies here, Tryptic peptides of extracted bands from SDS PAGE gels were analyzed by LC-MS/MS on a LTQ linear ion trap mass spectrometer coupled with a NanoLC pump and auto-sampler as previously described (Tang 2005). Peptides were eluted from the reverse-phase column into the mass spectrometer at 200 nL/min with acquisition time of either 49 or 75 min. To minimize carryover, a blank cycle was run between each sample. The mass spectrometer was set to repetitively scan m/z from 400 to 1600 followed by data-dependent MS/MS scans on the 3 most abundant ions with dynamic exclusion enabled.

Proteins were identified from MS/MS spectra using SEQUEST. DTA files generated from MS/MS spectra were searched against a human database (note: human samples were searched against IPI human database version 3.15). The databases were indexed with static modification of Cys by IAM, and additional dynamic modifications of Cys by either IAEDANS or mBBBr, and β -ME. Differential modification of Met to methionine sulfoxide was also considered. The peptides identified were assembled into the minimum number of unique proteins using SEQUEST SUMMARY. For reporting sequence coverage the data were filtered using $XCorr \geq 1.9$ ($z=1$), 2.2 ($z=2$), 3.75 ($z=3$) and $\Delta Cn \geq 0.1$. The extent of IAEDANS and IAM labeling at each site was determined from extracted ion chromatograms with identification of each specific Cys achieved through both the absolute mass of the modified-Cys peptide as well as the collision-induced dissociation mass fragmentation pattern. Ratios of IAEDANS to IAM labeling proved reproducible within about 10%.

Cleavage Pattern Verification of Cys labeling differences

To verify the differences in labeling detected by fluorescence, IAEDANS labeled ghost cells were treated with 2-nitro-5-thiocyanobenzoic acid (NTCB), which cleaves

peptide bonds selectively at reduced un-modified cysteines and therefore probes cysteine modification (Jacobson 1973). NTCB treatment of ghost cells reacted with IAEDANS under static or sheared conditions resulted in NTCB cleavage pattern differences that were both qualitatively and quantitatively distinct when analyzed by western blot (Fig. S1). Primary antibodies raised against β 16-17 detected additional bands in the static sample which are not present in the sheared ghost cell sample; likewise for antibodies against the N-terminal spectrin repeats α 1-5 (not shown). Thus, using two different readouts of labeling, we conclude that the application of shear stress results in an increase in cysteine labeling of spectrin.

Labeling of recombinant spectrin dimers versus monomers

Exposure to high levels of shear has been reported to alter the spectrin quaternary structure and dissociate the spectrin tetramer (An 2002). However, labeling experiments conducted on recombinant forms of the spectrin tetramer in the complexed and uncomplexed forms at 23° C and IAEDANS to protein ratios of 100:1 suggest that tetramer formation does not alter the labeling of cysteines and therefore can not account for the observed differences in labeling.

Refolding after labeling of recombinant spectrin

To address the structural effects of IAEDANS conjugation to Cys¹²⁰³ in α -R12, CD melting curves were measured on refolded protein which had been labeled under denaturing conditions. Measurements of the unconjugated protein yield a two-state melting profile with a $T_m = 36^\circ$ C (An 2006). By comparison, although IAEDANS-labeled α -R12 (designated by *) matched the melting profile at low temperatures, it displayed a slightly lower $T_m^* = 33^\circ$ C. This perturbation further suggests that the position of the cysteine is partially within the fold, but that conjugation has only a small localized effect on the overall structure of the protein and does not abrogate refolding after labeling.

Supplemental Analysis

The force-dependent Linderstrom-Lang (fLL) reaction scheme for labeling of sequestered sites to generate P(t) as given in the text leads to three rate equations ($\beta = 1/k_B T$):

$$\begin{aligned} dN/dt &= -k_{1r}e^{\beta f \Delta x} N + k_{1r}e^{\beta f \Delta x^*} U \\ dU/dt &= k_{1r}e^{\beta f \Delta x} N - k_{1r}e^{\beta f \Delta x^*} U - k_2 c U \\ dP/dt &= k_2 c U \end{aligned} \quad \text{Eq. S1}$$

Initially, $P = 0$ and $U \cong 0$ until force is applied. Also, the labeling dye concentration, c , is generally used in large excess (at mM). This set of coupled ordinary differential equations analyzed many years ago by Hvidt (1964; see Qian 1999) has a complex but tractable solution for $N(t)$, $U(t)$, and $P(t)$ that is given Fig. S5A and illustrated for relevant parameters in Fig. S5B. In one simple limit, refolding is negligible ($k_{1r} = 0$), and the solution reduces to that of the classic unidirectional ($N \rightarrow U \rightarrow P$). To compare with experimental kinetics that are well-fit by first order kinetics, we also fit our $P(t)$ to obtain the effective first order rate constant and generally find $R^2 > 0.95$.

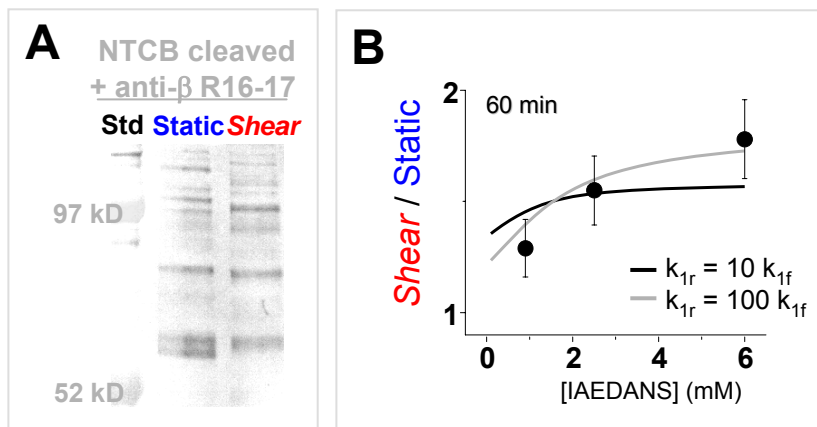
For static samples, the first equilibration is unimportant and so $P_{st}(t) = A [1 - \exp(-k_2 c t)]$. Based on fits of experiments in Fig.3A, $A = 1$ and $k_2 c = (7.5 \text{ min})^{-1} = 0.13 \text{ min}^{-1}$. For sheared samples labeled with a single dye (IAEDANS), the total amount of labeled protein is $P_{tot}(t) = P_{st} + P_{sh}$; in contrast, the sequential n-dye labeling method (Fig. 3B) largely eliminates the first term, and $P_{sh}(t)$ is given by the solution to the fLL equation (with $\max(P_{sh}) = 0.7 \max(P_{st})$). For the latter, fits of both the 60 min labeling and stress-dependent kinetics in Fig. 3B, we use the same $k_2 c = 0.13 \text{ min}^{-1}$. Reasonable fitting of the data (all at 37 °C) is obtained with $k_{1f} = 0.004 \text{ min}^{-1}$, $k_{1r} = 0.04 \text{ min}^{-1}$, and $\Delta x = 2.5 \text{ nm}$ and $\Delta x \leq -2.5 \text{ nm}$ based on estimates from AFM studies of forced unfolding of spectrin (Lee 2001; Law 2003); we also estimate the picoNewton forces (0 – 6.5 pN) on spectrin from the shear stress σ (0 – 1.7 Pa) as $f = \alpha \sigma$, where $\alpha = (1.95 \text{ }\mu\text{m})^2$ is 2-3% of average RBC surface area and of course reflects an average stressing dimension in shear. These order of magnitude estimates of parameters are of course being fit to multiple spectrin domains with different T_m , etc. and all in an intact cell. The longer term challenge therefore is to make more precise site-specific determinations (with improvements needed in quantitative MS) in order to relate the molecular microenvironment in the cell to purified protein analyses. The current connection between single molecule forced extension and stress-driven unfolding in intact cells is nonetheless suggestive.

Finally, note that a ratio of labeling rates for folded and unfolded states relates – with appropriate qualification (eg. Ha 1998) – to the free energy difference between folded and unfolded states. Here, the site-specific ratios from LC-MS/MS of $\phi \approx 5 - 10$ (60 min at 37 °C, 0.93 Pa in Table S1) agree with two-dye labeling results at a similar stress (Fig. 3B, top) and happen to be taken at a timepoint which is within an order of magnitude of stress-dependent reaction time constants. As such these ratios provide first crude estimates of $k_B T \ln \phi \sim 5\text{-}10 \text{ pN nm}$ for the range of irreversible work done in forced unfolding *in situ*. While this range is consistent with unfolding by picoNewton forces acting over nanometers, Fig. 3C (bottom) shows more rigorously that the effective rates of multi-site labeling are not labeling rate limited (at 0.93 Pa) and differ in *Shear* and *Static* samples by a ratio of 10 – 20:

$$k_{\sigma=0.93 \text{ Pa}} / k_{\sigma=0 \text{ Pa}} \approx (0.0015 - 0.003 \text{ min}^{-1}) / (0.03 \text{ min}^{-1}) = 330\text{-}660 \text{ min} / 33 \text{ min}$$

Since refolding is also shown to be of minimal importance, this ratio indicates a stress-dependent suppression of the forward barrier to unfolding by 9-12 pN nm.

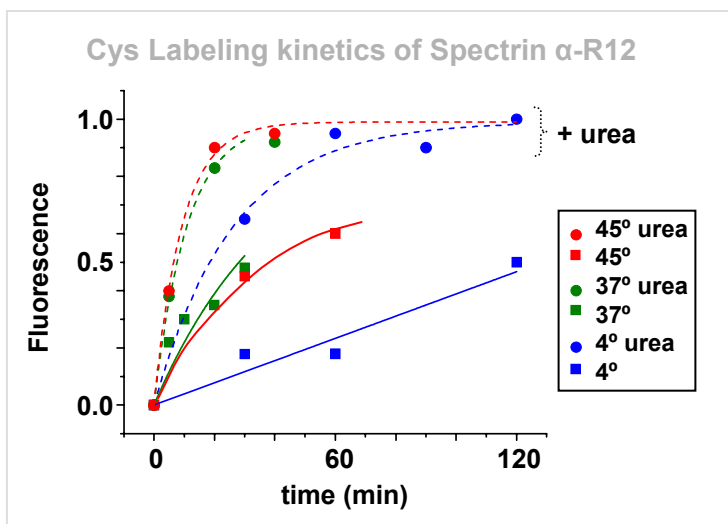
Figure S1



Differential labeling is site-specific and also depends on IAEDANS concentration.

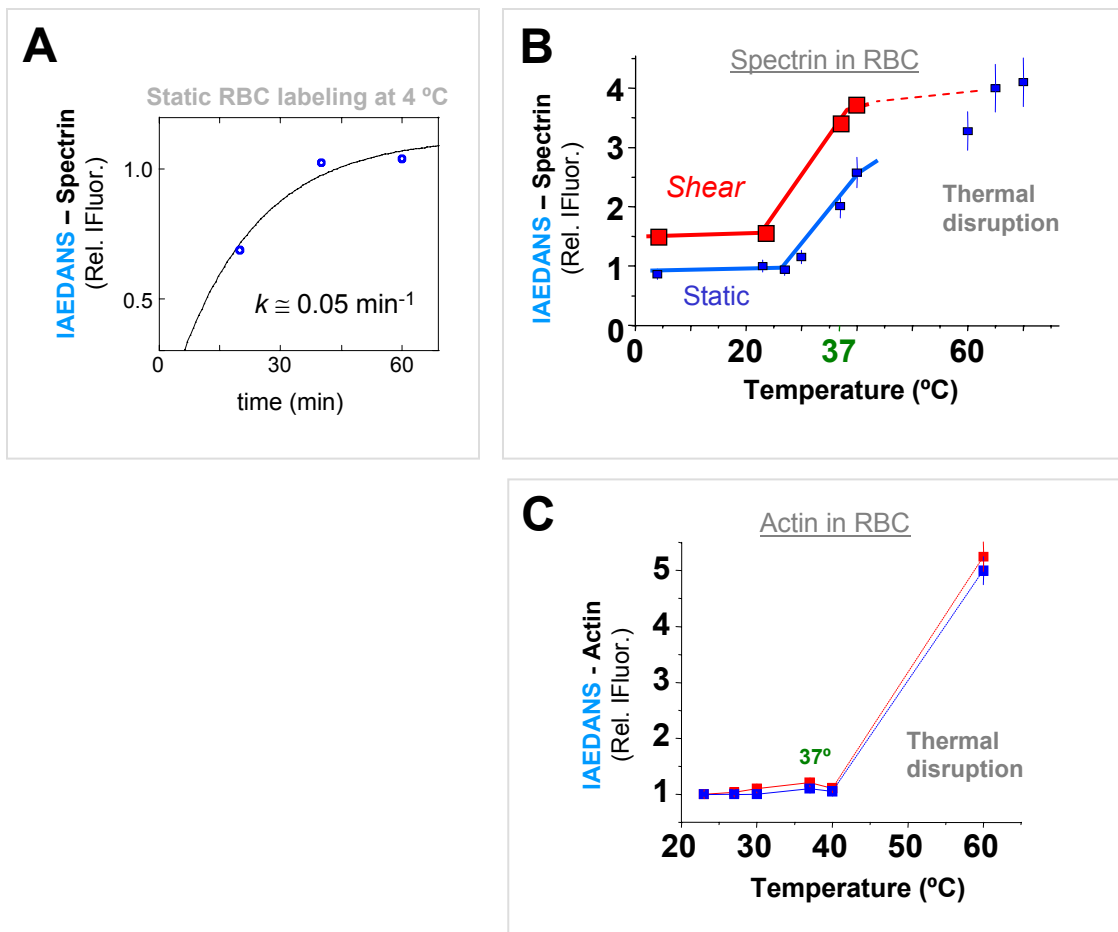
(A) Western blot of static and shear ghost cell spectrin treated with 2-Nitro-5-thiocyanobenzoic acid (NTCB). NTCB cleaves peptide bonds selectively at reduced un-modified cysteines, and therefore can be used as a probe of cysteine modification (Jacobson 1973). The NTCB cleavage pattern differs in both qualitative and quantitative ways probed with antibodies raised against the N-terminal spectrin repeats α 1-5. (B) Concentration dependence of the *Shear / Static* labeling ratio at 0.93 Pa, with fits to the fLL scheme using parameters in the Supplemental Analysis. For the higher refolding rate, $\Delta x = |\Delta x'| = 3$ nm and $max(P_{sh}) = max(P_{st})$. Error bars indicate experiments performed twice or more.

Figure S2



IAEDANS labeling kinetics for recombinant α -R12. Native (squares) and denaturing (circles) conditions were studied at various temperatures. The difference in labeling rates for native $k_N(T)$ and denatured $k_D(T)$ states relates to the steric protection of the lone Cys when folded. The weak increase in reaction rate in urea with heating reflects the usual Arrhenius-acceleration (2-3 fold per 30 K) and is independent of folding.

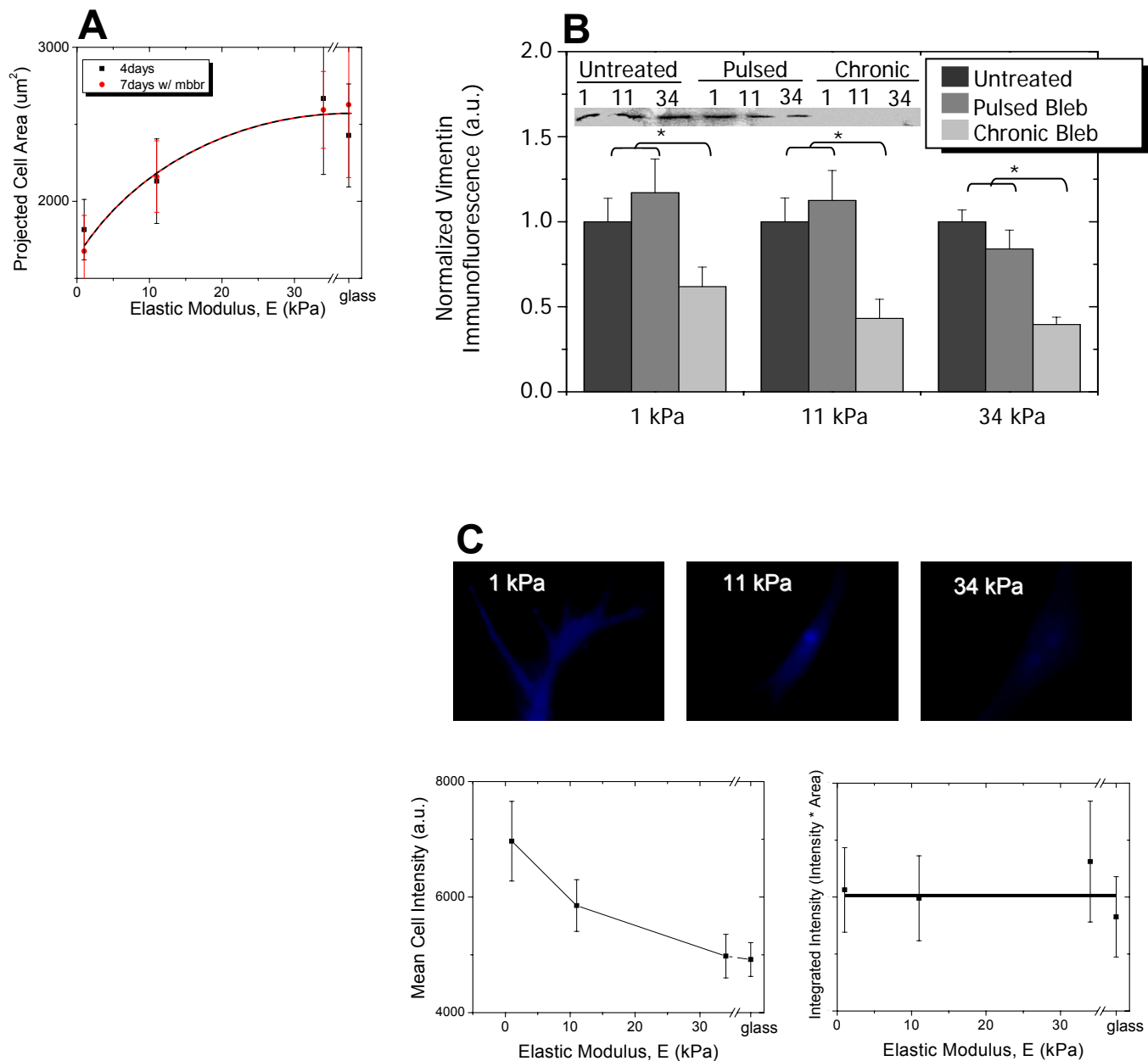
Figure S3



Temperature dependence of spectrin and actin IAEDANS labeling within RBC ghosts.

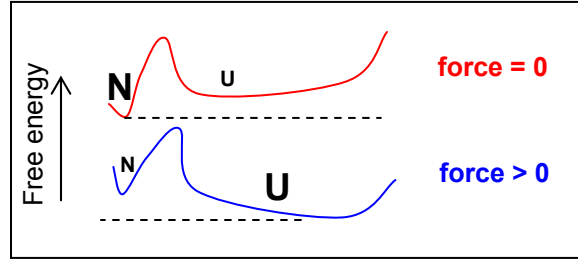
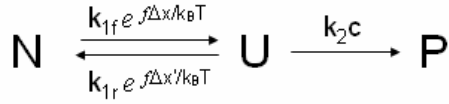
(A) Kinetics of spectrin labeling within static RBC ghosts at 4° C. Note that this rate is about 40% of the labeling rate at 37°C given in the text, which is consistent with typical temperature effects on reactions in solution. (B, C) Spectrin and Actin labeling after 60 min under either static or shear stress conditions. Spectrin labeling depends on temperature and shear stress (0.93 Pa), but Actin labeling is independent of shear stress and independent of temperature until thermal disruption of cells. Compared to previously measured loss of helicity in RBC membranes from Circular Dichroism (CD) (Jackson 1973), our static labeling profile is shifted to lower temperature in part because ours is a time-integrated result. In addition, the CD assesses all types of integral and peripheral membrane proteins. Error bars indicate results from experiments done twice or more.

Figure S4



Labeling effects on MSC. (A) Projected spread cell area with and without mBBR labeling, which reveals no differential in cell area under mBBR labeling. (B) Vimentin immunofluorescence intensity in MSC as a function of polyacrylamide substrate stiffness. At all stiffnesses tested, 24 hr blebbistatin treatment (“Chronic”) decreased overall intracellular vimentin concentrations, while 1hr incubation with blebbistatin (“Pulsed”) had no effect. Western blot staining (top inset) against vimentin shows a similar trend, with long term blebbistatin treatment resulting in decreased vimentin cellular concentrations (protein load per lane is constant). Quantitative fluorescence intensity measurements of mesenchymal stem cells on polyacrylamide surfaces of differing stiffnesses. Error bars indicate S.E.M. for analyses of at least 50 cells. (C) Representative images of mBBR treated MSCs plated on 1, 11, and 34kPa polyacrylamide surfaces. Plots of mBBR cell fluorescence intensity vs. substrate stiffness and of a constant cell-integrated mBBR intensity as a function of substrate stiffness. The latter result illustrates the measurements in (B).

Figure S5A



Solution to the force-dependent Linderstrom-Lang (fLL) Reaction Scheme with simplified notation: ($k_{1f}e^{f\Delta x/k_B T} \rightarrow k_{1f}e^f$), ($k_{1r}e^{f\Delta x'/k_B T} \rightarrow k_{1r}e^{f'}$), ($k_2c \rightarrow k_2$)

$$A = k_2^2 + 2k_2k_{1r}e^{f'} - 2k_{1f}k_2e^f + (k_{1r}e^{f'})^2 + 2k_{1f}k_{1r}e^{f+f'} + (k_{1f}e^f)^2$$

$$N(t) = \frac{C}{2\sqrt{A}} \left\{ k_2 \left(e^{-\frac{1}{2}t(k_2+k_{1f}e^f+k_{1r}e^{f'}-\sqrt{A})} - e^{-\frac{1}{2}t(k_2+k_{1f}e^f+k_{1r}e^{f'}+\sqrt{A})} \right) \right. \\ \left. + k_{1f}e^f \left(e^{-\frac{1}{2}t(k_2+k_{1f}e^f+k_{1r}e^{f'}+\sqrt{A})} - e^{-\frac{1}{2}t(k_2+k_{1f}e^f+k_{1r}e^{f'}-\sqrt{A})} \right) \right. \\ \left. + \sqrt{A} \left(e^{-\frac{1}{2}t(k_2+k_{1f}e^f+k_{1r}e^{f'}-\sqrt{A})} + e^{-\frac{1}{2}t(k_2+k_{1f}e^f+k_{1r}e^{f'}+\sqrt{A})} \right) \right. \\ \left. - k_{1r}e^{f'} \left(e^{-\frac{1}{2}t(k_2+k_{1f}e^f+k_{1r}e^{f'}+\sqrt{A})} - e^{-\frac{1}{2}t(k_2+k_{1f}e^f+k_{1r}e^{f'}-\sqrt{A})} \right) \right\}$$

$$U(t) = \frac{Ck_{1f}e^f}{\sqrt{A}} \left(e^{-\frac{1}{2}t(k_2+k_{1f}e^f+k_{1r}e^{f'}-\sqrt{A})} - e^{-\frac{1}{2}t(k_2+k_{1f}e^f+k_{1r}e^{f'}+\sqrt{A})} \right)$$

$$P(t) = Ck_2k_{1f}e^f \left(\frac{e^{-\frac{1}{2}t(k_2+k_{1f}e^f+k_{1r}e^{f'}-\sqrt{A})}}{\sqrt{A} \left(-\frac{1}{2}k_2 - \frac{1}{2}k_{1r}e^{f'} - \frac{1}{2}k_{1f}e^f + \frac{1}{2}\sqrt{A} \right)} \right. \\ \left. - \frac{e^{-\frac{1}{2}t(k_2+k_{1f}e^f+k_{1r}e^{f'}+\sqrt{A})}}{\sqrt{A} \left(-\frac{1}{2}k_2 - \frac{1}{2}k_{1r}e^{f'} - \frac{1}{2}k_{1f}e^f - \frac{1}{2}\sqrt{A} \right)} \right) + C$$

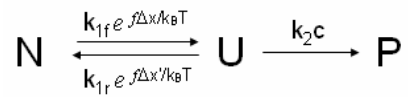
Reduction of Solution above to Unidirectional Reaction ($N \rightarrow U \rightarrow P$) with simplified notation: ($k_{1f}e^{f\Delta x/k_B T} \rightarrow k_{1f}$), ($k_{1r} = 0$), ($k_2c \rightarrow k_2$)

$$N(t) = Ce^{-tk_{1f}}$$

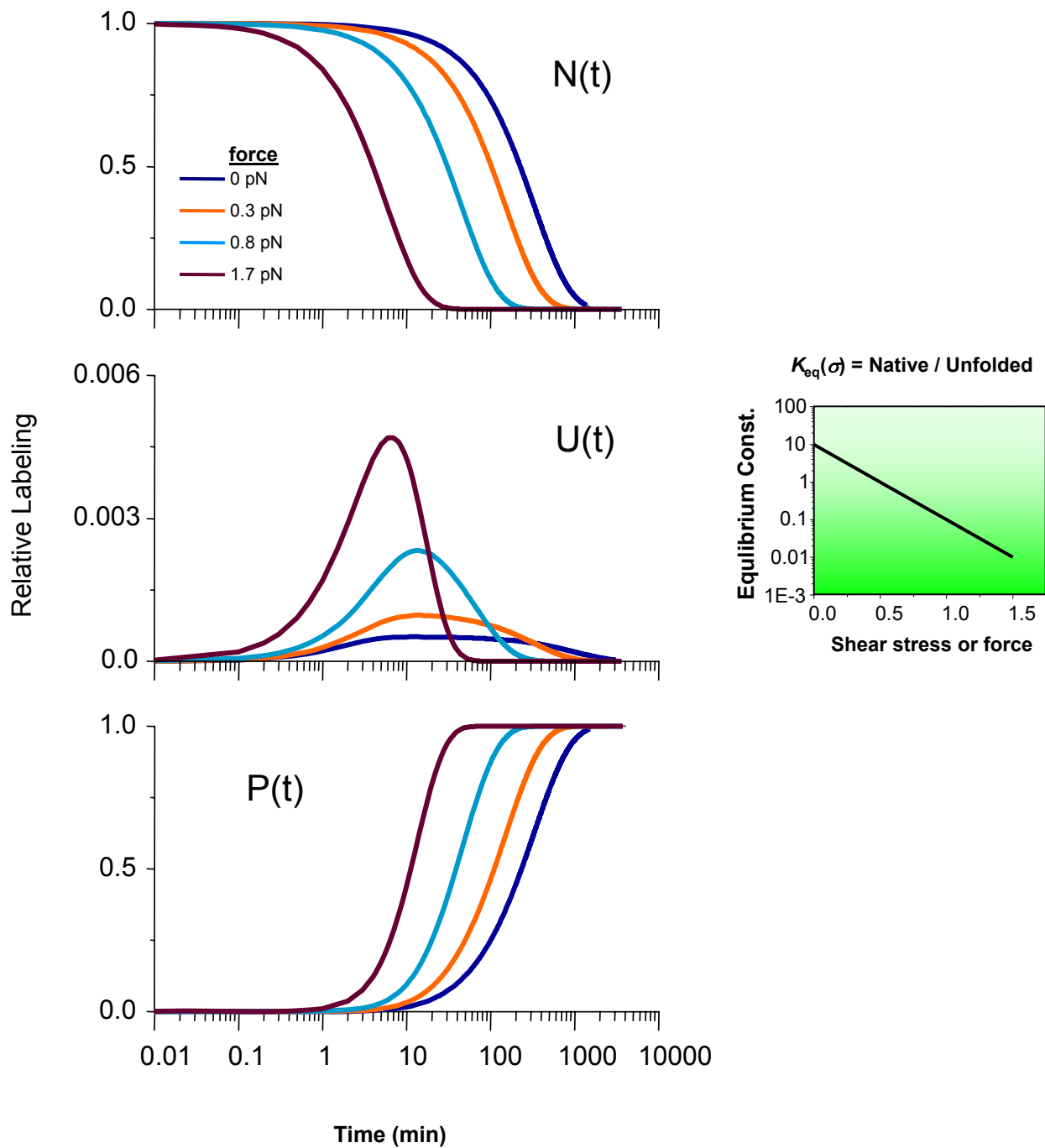
$$U(t) = \frac{Ck_{1f}}{(k_2 - k_{1f})} \left(e^{-tk_{1f}} - e^{-tk_2} \right)$$

$$P(t) = \frac{C}{k_2 - k_{1f}} \left(-k_2e^{-tk_{1f}} + k_{1f}e^{-tk_2} \right) + C$$

Figure S5B



Calculated kinetics of labeling for $k_{1f} = 0.004 \text{ min}^{-1}$, $k_{1r} = 0.04 \text{ min}^{-1}$, $k_2 c = 0.13 \text{ min}^{-1}$, $\Delta x = 2.5 \text{ nm}$, $\Delta x' = -2.5 \text{ nm}$



Supplemental Tables

Table S1-A LC-MS/MS results for labeled Cys in α -spectrin within RBC (60 min at 0.93 Pa shear, 37 °C). Y indicates detected; N.D. is not detected. $\phi \geq 2.0$ or $\phi \leq 0.5$ indicate significant differences. The overall average ratio of 2.6 assumed a unit ratio for the N.D. data.

	Repeat	$c = [\text{IAEDANS}]$	Shear labeled	Static labeled	$\phi = \text{Shear/Static}$
$\alpha 167$	R2	6 mM	Y	Y	$0.12 / 0.06 = 2.0$
$\alpha 224$	R2	6 mM	Y	Y	$1.27 / 0.19 = 6.4$
$\alpha 475$	R4	6 mM	Y (100%)	Y (100%)	1.0
$\alpha 773$	R7	6 mM	Y (100%)	Y (100%)	1.0
$\alpha 799$	R8	6 mM	Y	Y	1.0
$\alpha 965$	R9	2.5 mM	Y	Y	$1.9 / 2.8 = 0.67$
$\alpha 1203$	R12	2.5 mM 6 mM	Y	Y	$0.20 / 0.04 = 5.0$ $11.9 / 1.2 = 9.9$
$\alpha 1846$	R18	6 mM	Y	Y	1.1
$\alpha 1879$	R18	6 mM 6 mM	Y	Y	$3.8 / 0.53 = 7.2$ $14.5 / 1.95 = 7.4$
$\alpha 2059$	R20	2.5 mM	Y	N.D.	--
$\alpha 2071$	R20	6 mM	N.D.	Y	--
$\alpha 2101$	R20	0.9 mM	Y (100%)	Y (100%)	1.0
$\alpha 2156$	R21	6 mM	Y	Y	1

Table S1-B Distinctively labeled Cys in RBC β -spectrin from LC-MS/MS. Y indicates detected; N.D. is not detected. $\phi \geq 2.0$ or $\phi \leq 0.5$ indicate significant differences.

	Repeat	$c = [\text{IAEDANS}]$	Shear labeled	Static labeled	$\phi = \text{Shear/Static}$
$\beta 116$	CH1*	6 mM	Y (100%)	Y (partial)	>1.0
$\beta 187$	CH2	6 mM	Y (100%)	Y (100%)	1.0
$\beta 603$	R3	6 mM	Y	Y	0.8
$\beta 607$	R3	6 mM	Y (partial)	Y (partial)	$6 / 3.4 = 1.8$
$\beta 622$	R3	6 mM	Y (partial)	Y (partial)	$0.67 / 0.25 = 2.6$ $0.96 / 0.64 = 1.6$
$\beta 734$	R4	0.9 mM	Y (partial)	N	N.D.
$\beta 964$	R7	6 mM	Y (100%)	Y (partial)	>1.0
$\beta 967$	R7	6 mM	Y (partial)	Y (partial)	N.D.
$\beta 1167$	R9	6 mM	Y (partial)	Y	$3.0 / 0.33 = 11$
$\beta 1283$	R10	6 mM	N	N	1.0
$\beta 1556$	R12	6 mM	Y (100%)	Y (100%)	1.0
$\beta 1891$	R15	6 mM	Y	Y	$1.1 / 0.03 = 36$
$\beta 1896$	R15	6 mM	Y (partial)	Y (partial)	N.D.
$\beta 1961$	R16	6 mM	Y (partial)	Y (partial)	N.D.
$\beta 2011$	R17	6 mM	Y (100%)	N.D.	N.D.

*CH denotes a calponin homology domain.

Table S2 Cytoskeletal Proteome of MSCs cultured on an Elastic Matrix. Differentials refer to Cys-labeling differences following Blebbistatin treatment per Fig.4B (...).

	# Peptides detected	%Sequence coverage	Differential in PAGE	mBBR-Cys [#] detected	not mBBR ** labeled Cys [#]	Differential in LC-MS/MS	
N.M. Myosin IIA (226 kDa)	690 (272)	50 (20)	Y (+13%)	90, 916, 987, 1378	171,568,693, 739	90	
N.M. Myosin IIB	11 (0)	4					
N.M. Myosin IIC	21 (25)	3.4 (1)					
Filamin A***	538 (52)	50 (9)	Y (+7%)	574, 596, <u>717</u> , <u>1017</u> , 2067, 2159	477, 483, 1260, 2561	717, 1017	
Filamin B	121 (74)	4 (2)			2115,2501		
Filamin C	151 (18)	4.6 (3)					
Talin-1	41 (13)	9 (6)		2161			
Talin-2	5 (0)	2.3		13	2197		
α II Spectrin (brain)	179 (67)	13 (5)		315		1879 [†]	
β II Spectrin (brain 1)	62 (59)	13.2 (10)		604		622 [†] , 1892 [†]	
Tubulin α 3	40 (24)	23 (11)		347			
Tubulin β 2	59 (37)	29 (20)		12, 354			
Myoferlin	146 (44)	5 (1)					
Fibrillin	4 (0)	1					
Vimentin (53 kDa)	534 (455)	59 (47)	Y (-9%)	<u>327</u> *		327*	
Actin (α , β , γ)	51 (47)	8.1 (3)	Y (-7%)				
Rho GTPase prot.1	16 (5)	3 (1)					

* There is only one Cys in Vimentin.

[†] Based on location of labeled Cys in ~60% identical α I and β I Spectrins of Tables S1.

** IAM and β -Me labeled Cys since no unlabeled form detected.

*** Initial studies of Filamin A (from F. Nakamura) in gels with F-actin show enhanced IAEDANS labeling in rheometer-sheared gels.

Supplemental References (in order of citation)

- An X, Lecomte MC, Chasis JA, Mohandas N, Gratzer W. Shear-response of the spectrin dimer-tetramer equilibrium in the red blood cell membrane. *J Biol Chem*. 2002 277(35):31796-800.
- Roth AF, Wan J, Bailey AO, Sun B, Kuchar JA, Green WN, Phinney BS, Yates JR 3rd, Davis NG. Global analysis of protein palmitoylation in yeast. *Cell* 2006 Jun 2;125(5):1003-13.
- Tang HY, Ali-Khan N, Echan LA, Levenkova N, Rux JJ, Speicher DW. A novel four-dimensional strategy combining protein and peptide separation methods enables detection of low-abundance proteins in human plasma and serum proteomes. *Proteomics* 2005 5(13):3329-42
- Jacobson GA, Schaffer MH, Stark GR, & Vanaman TC. Specific chemical cleavage in high yield at the amino peptide bonds of cysteine and cystine residues. *J. Biol. Chem*. 1973 248(19):6583-91.
- Hvidt, A. A discussion of the pH dependence of the hydrogen-deuterium exchange of proteins. *Compt. Rend. Trav. Lab. Carlsberg*, 1964 34: 299-317.
- Qian H, Chan SI. Hydrogen exchange kinetics of proteins in denaturants: a generalized two-process model. *J Mol Biol*. 1999 286(2):607-16.
- Jackson WM, Kostyla J, Nordin JH, Brandts JF. Calorimetric study of protein transitions in human erythrocyte ghosts. *Biochemistry* 1973 12(19):3662-7.